Influence of applied coating time on nano hydroxyapatite/chitosan coating on 316L stainless steel alloy using electrophoretic deposition for biomedical application

Aya Muhsun Hazber[1]*, Ayad Naseef Jasim[1], Jabbar Qassim Gattmah[1], Jaber Kasem Kutm[1], Fatemeh Poorsalehi[2]

[1] Material Engineering Department, University of Diyala, Iraq
[2] Department of Chemistry, Amirkabir University of Technology, Tehran, Iran
* Corresponding author's e-mail: engayo53@gmail.com

ABSTRACT

In this work, an electrophoretic deposition (EPD) method was utilized to cover a biocompatible stainless steel medical grid type 316L with nanoparticles of hydroxyapatite (HA). ln conjunction with the biopolymer chitosan (CHT), as a binder, it enhances the adhesive capabilities of a substrate. The chosen bio-coating method is the EPD process of 316L Stainless Steel alloy due to its ease of use, low cost, and capacity to coat intricate items. Consequently, this research studied different concentrations of the materials utilized, the most significant variables, and their effects in order to acquire the optimal attributes for the coating layer, using voltage applied and deposition time. The coating periods were 2, 4 and 6 minutes, and the concentrations were 4, 7 and 10 g/L, while the voltages were modulated between 20, 40, and 60 volts. In spite of the fact that the metallic medical applications and bone replacement have made substantial and fruitful progress, difficulties still persist. The coating procedures have a significant impact on how well the composite materials work in the biological devices. To improve the properties of composites used in biomedicine, coating them is an essential step. X-ray diffraction (XRD) spectroscopy and scanning electron microscopy (SEM) were used to examine the deposited coatings, and the Zeta potential for suspensions was computed.

Keywords: biomedical, hydroxyapatite, electrophoretic deposition, 316 stainless steel, chitosan, XRD, SEM.

INTRODUCTION

Bioactive material coatings on the metallic implants have recently attracted a lot of attention. The majority of orthopedic implants are composed of metal alloys, as titanium alloys and stainless steel. It is worth noting that 316L stainless steel has found extensive usage in the orthopedic industry. This is because of how strong it is mechanically, simultaneously being affordably priced. There is a dearth of this metallic alloy in the implantation sector, despite its many benefits. The metal is probably encased in fibrous tissue, and its surface might release some harmful ions into the bloodstream [1, 2]. This may cause the metallic implant to shift and become loose [1, 3]. An allergy may manifest itself in response to the typical corrosion products of stainless steel, which include nickel, cobalt, chromium, and their compounds [4]. It is reasonable to anticipate that the osteoblast-like bone marrow cells will exhibit improper behavior, even at low quantities [4]. As a result, it is critical to develop ways for reducing the corrosion products of such implants in the harsh body environment. Coating the metallic implants with a bioactive layer has been suggested as an effective solution to address this issue. Within this framework, the bioactive glass [5–7] and glass-ceramics [8–10] EPD is widely employed as an economical and straightforward technique for several coating applications [11, 12]. Plasma spraying deposition, electrostatic

spray deposition, and pulsed laser deposition are three more technologically used methods for calcium phosphate coating [13, 14]. However, such methods as DC and AC electrophoretic depositions use a direct current (DC) field or an alternating current (AC) field to supply the voltage that is exposed to the electrophoresis in the same way [15]. The deposition of charged particles in suspension onto an electrode with an opposite charge occurs under the influence of a set electric field in the direct current-electrophoretic deposition technique. A technique called alternating current electrostatic deposition involves regularly inverting the direction of the electric field [2]. This is what causes the powder particles in suspension to oscillate and migrate between the electrodes. In electrophoretic deposition, the asymmetry and wave frequency determine the oscillating migration [16–18]. The great bio-compatibility and close chemical similarity of hydroxyapatite (HA) to natural bone tissues led to its extensive use in dentistry and medical applications; Hazim et al. (2017) [19] coated the 316L stainless steel substrate with a nano bio-composite of bio-ceramics using an EPD. As a coating with the bio-polymer (chitosan) matrix, the nano HA and nano YSZ with FGMs have been employed and used to install FGM bio-composite coatings and single coatings at different parameters, such as voltage, duration, and percentage concentration of powders. The positive results for the antibacterial activity were demonstrated by the FGM samples. Adnan (2016) [20] created a coating layer via EPD using YSZ and HA on the stainless steel 316L with chitosan acting as a binder for the substrate. At 30 V and 5 minutes, the findings demonstrated that the microstructure in the isopropanol solution of YZS into HA was homogenous and devoid of cracks. Sorkhi et al. (2019) [21] coated 316L stainless steel with HAp-chitosan-titania nano-composite materials derived from methanolic and ethanolic solutions using the electrophoretic deposition (EDP) method. The depositions from an ethanolic mixture containing 0.50 g/L chitosan, 5 g/L titania, and 2 g/L HAP achieved the highest possible coating surface quality and corrosion resistance. Nuswantoro et al. (2019) [22] selected HA as the coating material to assess the bio-activity, bio-compatibility, and mechanical properties of this ceramic material. The two most important elements affecting the EPD process so far were the coating duration and voltage. Coating thickness, mass growth, and surface coverage were all shown to increase, as the coating duration and voltage were increased. Drevet et al. (2015) [23] examined the process of EPD of a nano-sized powder as it pertains to the production of hydroxyapatite coatings. Two crucial experimental factors, the potential and the deposition time, were investigated in this study. The coating was ideally deposited at 10 V for 10 minutes for the optimal results. The thermal treatment of samples in a controlled environment was then applied after the electrophoretic deposition to improve their mechanical characteristics, essential factors to prolong the life of implant materials. To create nano-HA coatings with the right dimensional characteristics that are known to enhance the biological response, a new synthesis method was devised. Also, Chen et al. 2014 [24] created a multilayered structure out of HA and biopolymer materials, like chitosan by combining the layer-by-layer fabrication with the EPD deposition, alginate, and polyvinyl alcohol. The layers that were deposited using EPD were organized as follows: A bottom layer of stainless steel, composite HAP, and alginate; a second layer of polyvinyl alcohol and alginate was deposited using the same procedure. The process of layer-by-layer deposition was finally employed to create the alginate and chitosan layers. Using a HA layer at the bottom resulted in a consistent rate of disintegration and great bioactivity, according to the data. In 2015, Frantiska et al. [25] investigated the HA and gelatin coatings using EPD on the SS substrates. Using colloidal processing, the HA particles were incorporated into gelatin. A Ti buffer layer was created and injected into the coating to enhance the strong connection between the stainless steel and the HA-gelatin layer. Because of the increase in suspension conductivity, thick layers have been achieved, EPD to coat 316L stainless steel with a chitosan/gelatin/hydroxyapatite mixture. The coating was shown to be cytocompatible, allowing osteoblast cells to proliferate and develop. Chitosan/gelatin/HA is a good choice for the biological applications because of its resistance to mechanical and chemical attacks. N. F. Nuswantoro et al. (2019) [27] employed the EPD to coat the HA nanoparticles onto the biocompatible titanium alloy Ti6Al4VIn in order to increase its bioactivity. The voltages were set to 3, 5, and 7 volts, with coating durations of 3, 5, and 7 minutes. The best HA coating that met the criteria for orthopedic implants was obtained by applying 5 volts for 5 minutes.

EXPERIMENTAL WORK

Materials

The material used in this research prepared as a plate was stainless steel 316 L tested in Company for Inspection and Engineering Rehabilitation (SIER). Table 1 illustrates the chemical analysis of the used alloy.

The following materials were acquired from Sigma Aldrich: hydroxyapatite (40 nm, 99% purity, white hue, 3.140 g/cm^3 density), chitosan (medium molecular weight, 85% de acetylation, soluble in 1% acetic acid, > 98% purity), ethanol solution.

Preparation of samples and solutions

The stainless steel alloy was cut to (10 × 20 × 3) mm, (17 × 17 × 3) mm as shown in Figure 1, and then ground with SiC emery paper using 220, 400, and 600 grit. The cleaning process used ethanol in an ultrasonic bath for 15 min. Finally, the samples were dried at 100 °C inside an oven for 15 min. The aqueous suspension of HA was prepared by using ethanol. Then, the HA nanoparticles were added with ethanol solution.

Electrophoretic deposition cell

On the basis of the schematic EPD system depicted in Figure 2, the EPD cell utilized in this investigation comprised a beaker and two electrodes submerged in the suspension ethanol solution. Components of the EPD Instrument, included a digital power supply and copper wire. The anode and cathode were made of stainless steel 316L. Different deposition settings, including concentrations of 4,7 and 10 g/L of HAP, 2, 4, and 6 min, and voltages of 20, 40, and 60 volts, were

Table 1. Chemical analysis of 316 Stainless steel

Sample	C%	Si%	Mn	P%	S%	Cr%	Mo	Ni%	Cu%	Al%	Fe%
Remainder	0.0273	0.467	1.40	0.0296	0.0005	17.36	2.14	11.9	0.431	0.0042	Ball
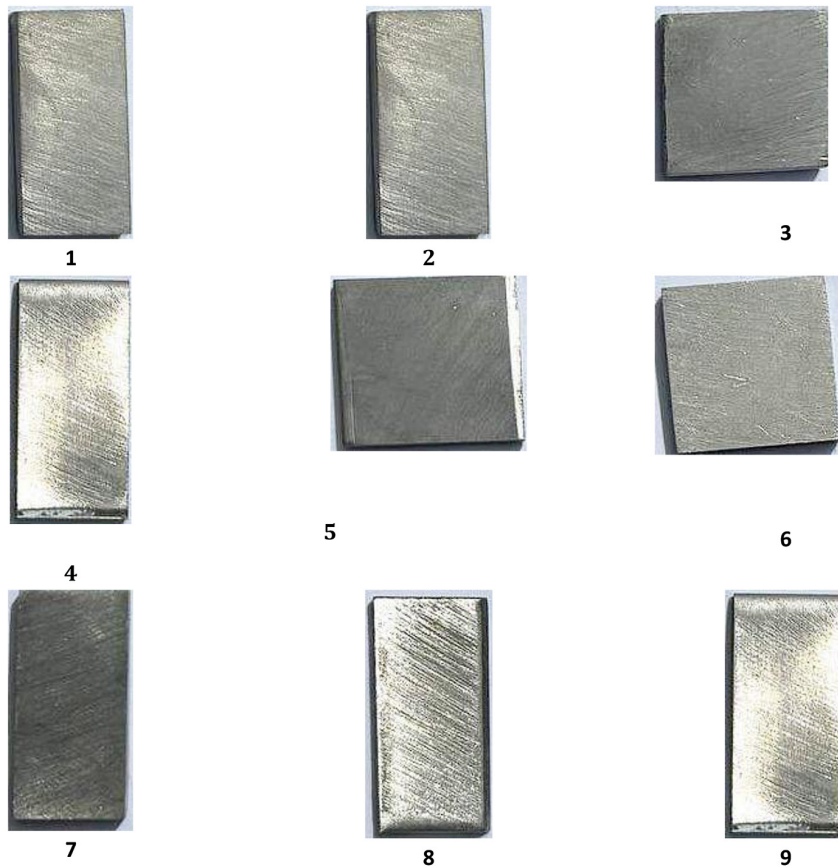
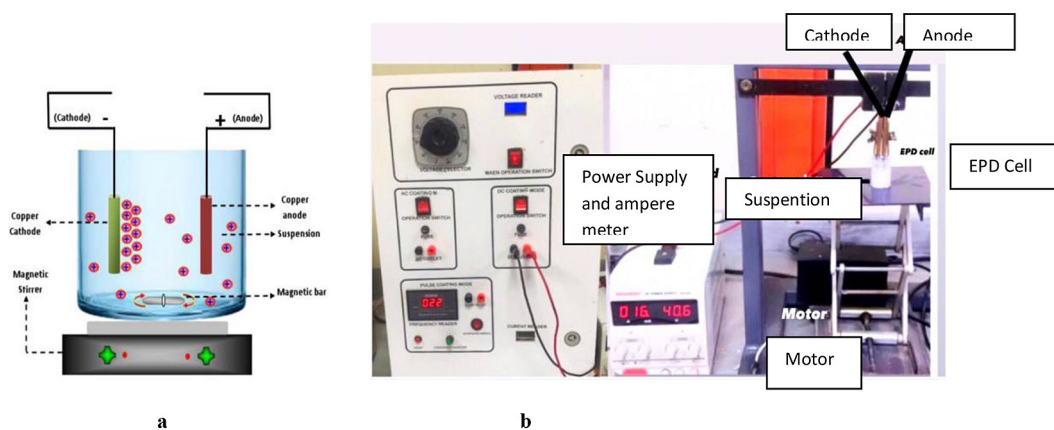**Figure 1.** Preparation of samples

Figure 2. (a) Diagram of the EPD system, and (b) EPD system

used to carry out the deposition procedure. the coating of the samples was subsequently dried by air while still at ambient temperature. Three different concentrations (4, 7, and 10 g/L) were used to create the EPD solution. Coating layers were formed using hydroxyapatite, which was acquired from Sigma Aldrich and has a particle size of 40 nm, a purity level of 99%, a white hue, and a density of 3.140 g/cm³. The chitosan that was bought from Sigma Aldrich has a medium molecular weight and is 85% deacetylated; it is soluble in 1% acetic acid and has a purity level of more than 98%. Stainless Steel 316L and HA particles were both bound with it. An essential part of conducting EPD experiments is preparing aqueous suspensions. The initial stage involved dissolving 0.06 g/L of chitosan in 1% acetic acid. Afterwards, 5% distilled water was added to the solvent, and finally, nano powder of HAP materials were added. A magnetic stirrer was used to de-agglomerate all of the solutions. Next, for half an hour, it was subjected to a high-powered sonicator (Ultrasonic Processor, MIXSONIX Incorporated N.Y., USA). The pH-DC-TDS Meter Portugal, which measures dissolved solids concentration, was calibrated using a pH meter that was pre-soaked with acetic acid. To guarantee the stability of each solution, its zeta potential was measured.

Figure 2 shows that a voltage or steady power source is linked to the holder of two electrodes. The electrodes in the beaker were raised and lowered using an electric stand that moved in accordance with the design of the cell deposition system. In order to conduct the studies, the coating was applied under the specified circumstances. The optimal deposition process parameters were found using the Taguchi technique. The objective was to determine the best set of controlling parameters so that the Taguchi technique performed the best while dealing with noisy circumstances factors. The hydroxyapatite layer was deposited experimentally using L9 (33) orthogonal arrays in this investigation. Table 2 shows the experiments that were planned using Taguchi's method, and Table 3 displays the parameters of the orthogonal array for HAP layer that were employed for these studies [28–29].

TAGUCHI RESULTS

The optimal conditions for preparing the HA layer on the Stainless steel 316L substrate were determined using Taguchi's statistical approach after the suspension preparation for HA prepetition. In order to have the thickest possible coating, the HAP layer must be prepared. To determine the coating thickness of a HA layer using DC current, the Taguchi design (L9) was employed. Ideal values for voltage (V), time (t), and concentration (C) [30] were selected according to the S/N ratio. When using EPD with DC current, the ideal values for HAP coating thickness are shown in Table 2.

DEVICES USED

Zeta potential test

The coatings and suspensions were investigated using zeta potential to guarantee their uniformity and stability. Zeta potential and electrophoretic mobility were determined using the laser doppler velocimetry (LDV) technique, using the Zetasizer Nano ZS instruments made by Malvern Instruments in the UK. At three different depths within the suspension, the computed zeta potential – a rate – was determined. Magnetic and

Table 2. L9(33)A HA layer orthogonal array

Experimental	Voltage (v)	Concentration (g)	Time (min)
1	1	1	1
2	1	2	2
3	1	3	3
4	2	1	2
5	2	2	3
6	2	3	1
7	3	1	3
8	3	2	1
9	3	3	2

Table 3. Deposition factors affect the HA layers

Sample-No.	Voltage (V)	Concentration(g/L)	Time (min)
1	20	4	2
2	20	7	4
3	20	10	6
4	40	4	4
5	40	7	6
6	40	10	2
7	60	4	6
8	60	7	2
9	60	10	4

ultrasonic stirring of the suspensions was performed for 10 minutes before to zeta latent measurement. Factors such as deposition duration, applied voltage, and suspension concentration might influence the coating quality in the EPD process, which in turn depends on the zeta potential [31]. Figure 3 shows the zeta potential device.

Atomic force microscopy (AFM)

To examine the morphology and roughness of the coating surface, the AFM method was employed, As shown in Figure 4, With a resolution value of around 1 nm or below, it is a method with extremely high value resolution. In this way, the AFM is a valuable tool for controlling matter on a nanometer scale. Using the AFM, the surface morphology of EPD films can be examined, which includes surface roughness and the ability to forecast changes in grain boundaries.

X-ray diffraction

X-ray diffraction (XRD) is a tool to identify crystalline phases from single or complex compositions. X-ray beams were emitted towards the sample surface and collide with the atoms of the samples. Only the deflected photos possessing the same wavelength as the incident X-ray photos would be gathered. If the Bragg's law was fulfilled, deflected X-ray beams reinforced each other and led to the called diffraction. The Bragg's law equation below.

$$n\lambda = 2dsin\theta \qquad (1)$$

RESULTS AND DISCUSSION

Solution stability (Zeta potential) results

Figure 5 shows that the zeta potential is positive at 25.70 mv and the mobility value is 2.01

Figure 3. Zeta potential device
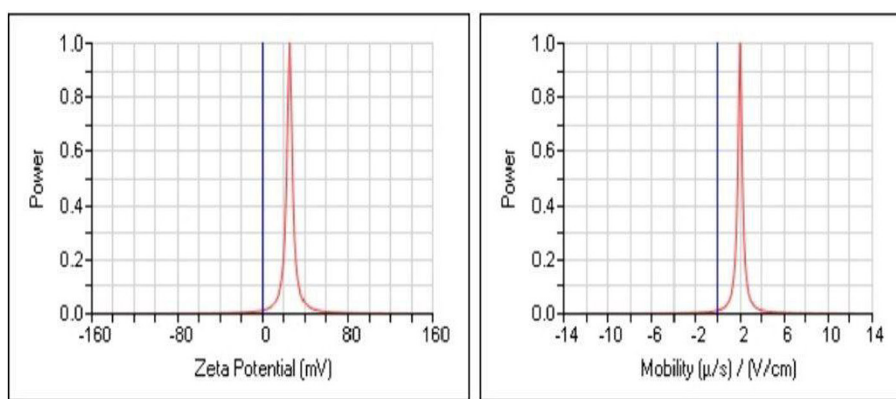
Figure 4. AFM device

Figure 5. Results of zeta potential for HA suspension

m/s, both of which contribute to the enhanced precipitation of homogenies HA. A higher absolute zeta potential results in more mobility. Due of their strong mobility, HA particles revert to a positive zeta potential [32].

Taguchi results

Following the HA suspension preparation, the optimal conditions for preparing the HAP layer on the stainless steel 316 L substrate were determined using the Taguchi statistical technique. The goal of preparing the HA layers was to obtain the maximum possible coating thickness. Table 4 and Figure 6 show that the optimal choice was the signal-to-noise ratio (S/N), which was determined by the higher values of V, t, and C. The findings for the thickness measurement of the HA layer using DC current were achieved according to the Taguchi design (L9), as indicated above Table 5 shows the ideal conditions for the thickness of the HA coating when utilizing an EPD with a DC current.

Surface morphology of HA coating on the sample surface

On the basis of the images shown in Figures 7 and 8, the surface morphology of the hydroxyapatite coating shows that it was homogeneous and uniform. The surface morphology of the samples seems to vary significantly. An optimally distributed HA coating may be achieved by adjusting the coating time. The HA coating is most evenly distributed throughout the surface of the 5-minute curing sample. The coated surface that comes into touch with the bone tissue is the crucial component.

Figure 7 shows the stainless steel samples that were subjected to the EPD coating process using hydroxyapatite. The first image is at a concentration of 4, the second sample at a concentration of 7, and the third at a concentration of 10. After drying the samples for 48 hours and performing the Taguchi method these samples are the best out of 27. Figure 9 shows the cross-section of samples. It was noticed that the

Table 4. Ratio of signal to noise

Sample number	Voltage (V)	Time (min)	Concentration (g/L)	Thickness (µm)	SNRA1	MEAN1
1	20	2	4	17.96	25.0861	17.960
2	20	4	7	19.58	25.8363	19.580
3	20	6	10	18.92	25.5384	18.920
4	40	2	7	20.29	26.1456	20.290
5	40	4	10	21.552	26.6698	21.552
6	40	6	4	19.805	25.9355	19.805
7	60	2	10	19.02	25.5842	19.020
8	60	4	4	18.63	25.4043	18.630
9	60	6	7	20.192	26.1036	20.192
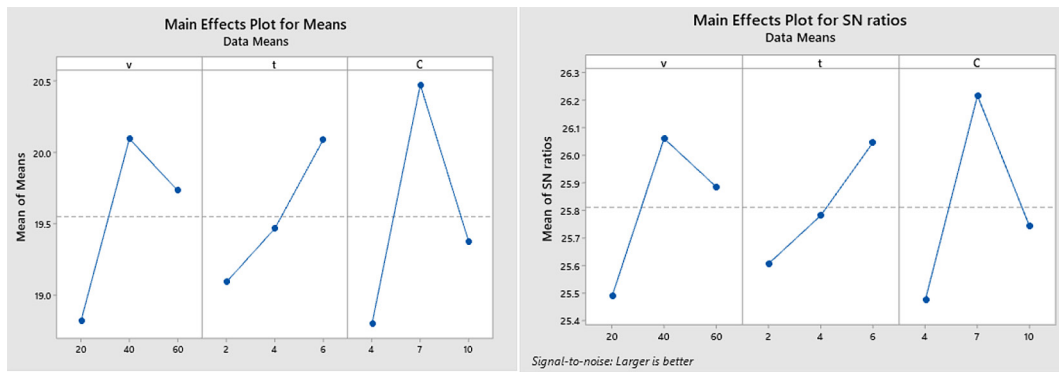
Figure 6. Ratio of signal to noise and means for thickness

Table 5. Using EPD with DC current to achieve the ideal condition for HA coating thickness

Thickness (µm)	Voltage (V)	Time (min)	Concentration (g/L)
Ratio of signal to noise	40	4	7
Means	40	6	10
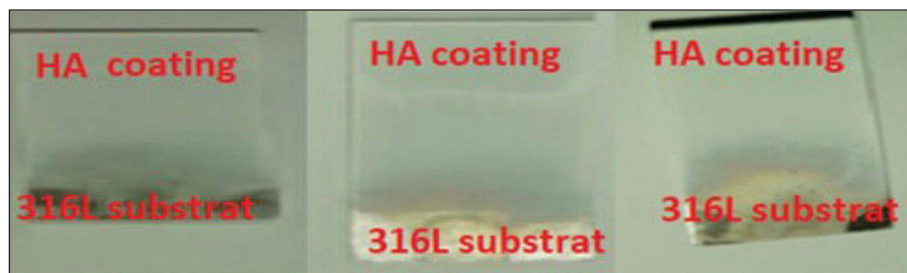
Figure 7. Sample coating with HA

thickness varies from one sample to another according to the conditions used (voltage, time and concentrations), as samples No. (1, 6, 8) have a concentration of 4 and the thickness value ranges between (17–19 micrometers), and samples No. (2, 4, 9) have a concentration of 7 and the thickness value ranges between (19–20 micrometers), and samples No. (3, 5, 7) have a concentration of 10 and the thickness value is (18–21 micrometers). After conducting the Taguchi method for coating hydroxyapatite on stainless steel, it was found that the best coating was achieved at (V = 40 v, t = 6 min, C = 7 g/L) This sample is very similar to sample No. 4 (voltage 40, time 2
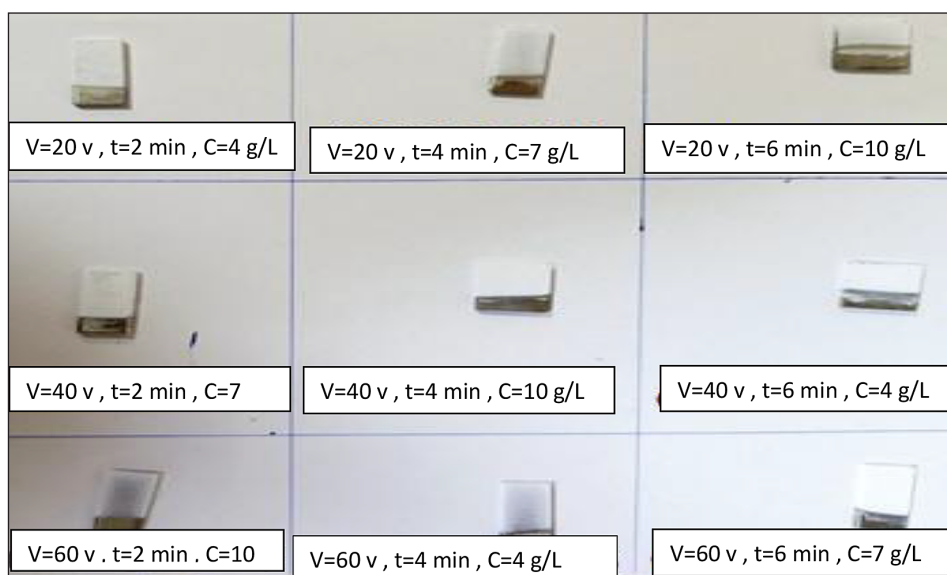
Figure 8. Optical images of the HA layer prepared according to the Taguchi method
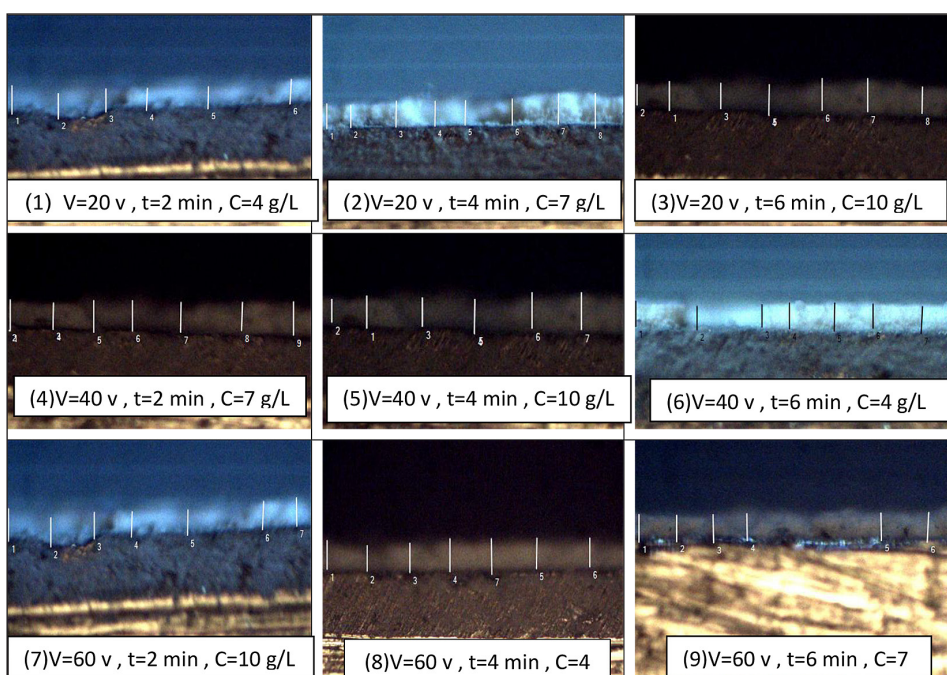

Figure 9. HA layer under optical microscopy according to the Taguchi method with coating thickness

minutes, concentration 7), which ensures a uniform, regular, homogenous coating which is free of cracks.

Analysis using atomic force microscopy (AFM)

In bone replacement applications, roughness is an essential component of the electrophoretic deposition (EPD) process. Roughness (49.66) and particle size (344.133) are the average roughness values for the coated hydroxyapatite substrates.

On the other hand, the AFM-measured nanoscale roughness is shown in Figure 10. In order to measure the roughness, a micrometer was utilized. Roughness of the 316L substrate surface and nanocomposites placed on it. By affecting adhesion, differentiation, and proliferation on the implant surface, this property ensures a secure connection to the host bone. The nanoparticles deposited on stainless steel 316L surfaces can take on a wide variety of shapes due to differences in the EPD settings [33].
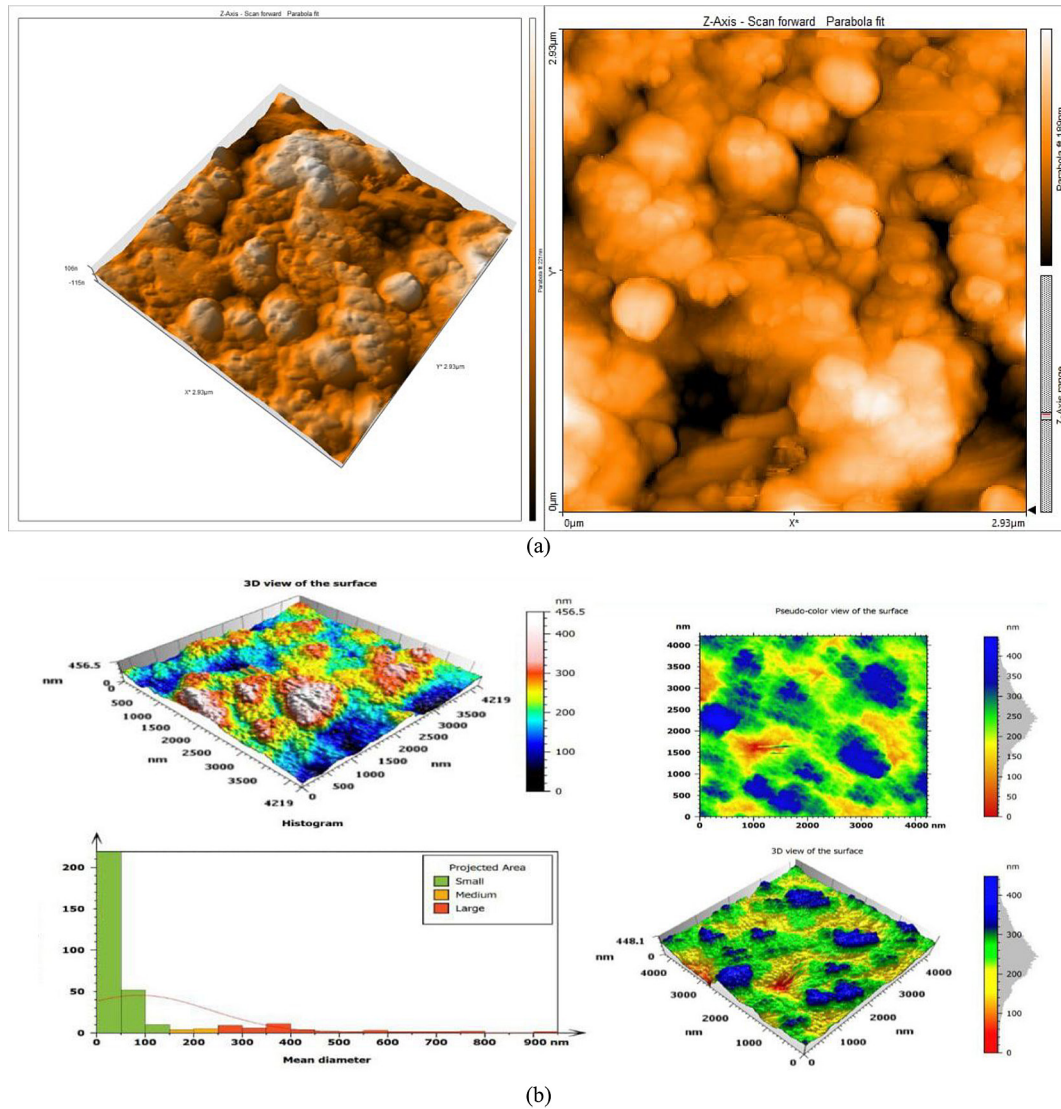
(a)

(b)

Figure 10. Two- and three-dimensional AFM images of the HA coating

X-ray diffraction analysis

The XRD for a single layer of hydroxyapatite deposited on the alloy substrate showed the presence of different diffraction peaks, as compared with powder of HA. This can be attributed to the chitosan particles, which act as a binder material and as a coating thin layer on stainless steel 316 L substrate which affected the XRD peaks. Figure 11 illustrates the phases of HAP layer. Figure 11a XRD analyses for stainless steel 316 L alloy, there are three different 2θ associated with 316L austenitic stainless steel [42.09° (111), 49.90° (200) and 74.08° (220)]. They were identified according to JCPDS Card No. 33-0397. In turn, Figure (11b) shows the hydroxyapatite phase-corresponding peaks as[(211) at 31.77, (300) at 32.90, (002) at 23.87, (222) at 42.7 and (213) at 49.46, according to Joint Committee

on Powder Diffraction Standards JCPDS card No. 09-0432. The highest intensity for HA was found at 2Ø 32.25º. The wider profile of the peaks may reveal lower crystallinity and/or small crystalline size of the nanoparticles. This helps to obtain a uniform and homogeneous coating layer.

Figures 11a and 11b show the XRD results of uncoated and coated SS 316L substrates. For the uncoated specimens of stainless steel 316L, the XRD pattern shows a single-phase solid solution of Fe, Cr, and Ni with an austenitic matrix phase (γ-FCC) structure. The peaks corresponding to the (110), (111), and (210) planes of the stainless steel 316L lattice are mentioned at different 2θ of 42.94, 49.90, and 74.08 degrees. The (111) plane is a commonly observed peak in FCC structures in which lattice parameter (a = 3.54Aˆ) and the average particle size equals 15.91 nm, while coated SS
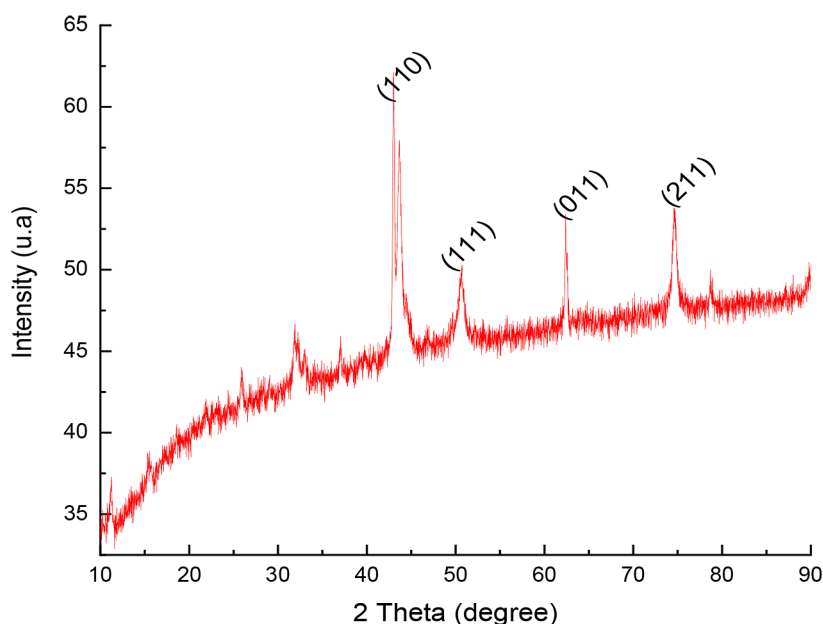
(a) XRD pattern of 316L stainless steel
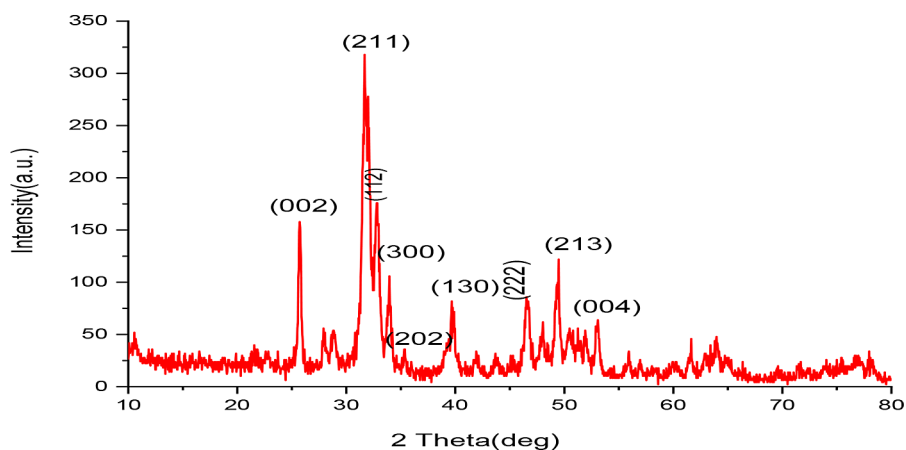
(b)XRD pattern of XRD-HA

Figure 11. XRD-analysis of the (a) S.S steel substrate and (b) HA

Table 6. Values of peacks of the XRD to pure 316 SS and HA

ITEM	2Theta (deg)	d (A)	FWHM (deg)	Intensity (Counts)	(hkl)
	42.94	2.11	0.57	81	110
Uncoated SS 316L	49.90	1.83	0.64	20	111
	74.08	1.28	0.52	17	210
	25.76	1.34	0.48	99	002
Coated SS 316L with HA	31.83	1.73	0.84	165	211
	39.88	2.16	0.5	87	130

316L substrate also indicates the presence of nano-hydroxyapatite peaks. These peaks correspond to the nanocoating layer, the specific (hkl) indices mentioned for the nanohydroxyapatite peaks are (002), (211), (130), and (213) corresponding to 25.76, 31.83, 39.77, and 49.68, respectively, according to the JCPDS card No (33-0397). The (111) plane is commonly observed; it crystallizes

in a hexagonal structure that lattice parameter (a = 9.41Å) and (c = 6.881Å) and the average particle size equals to 14.46 nm. The results of x-ray diffraction examination of the coated sample confirm the disappearance of all the SS 316L alloy phases, which confirms the complete coverage of the hydroxyapatite coating material of the alloy surface.

Analysis using scanning electron microscopy (SEM)

The surface layer structure of the multilayer composite coating was determined using SEM. The uniform dispersion of particles allowed for the production of a uniform coating, at a high
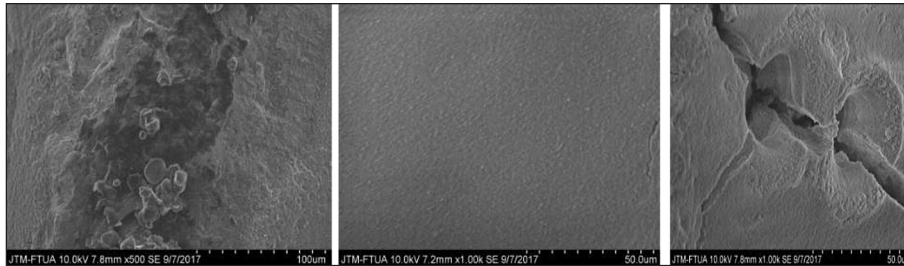

Figure 12. SEM imaging of surface morphology of HA coating on surface at different time
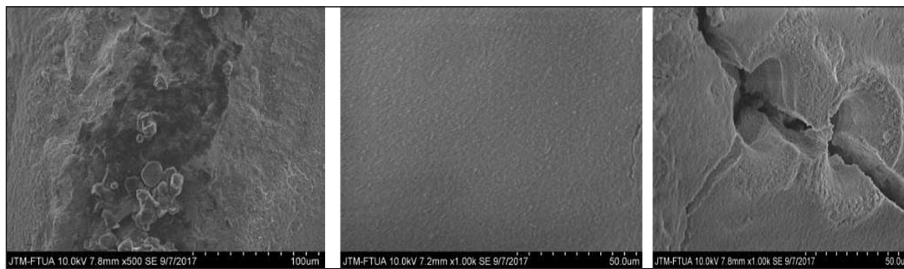

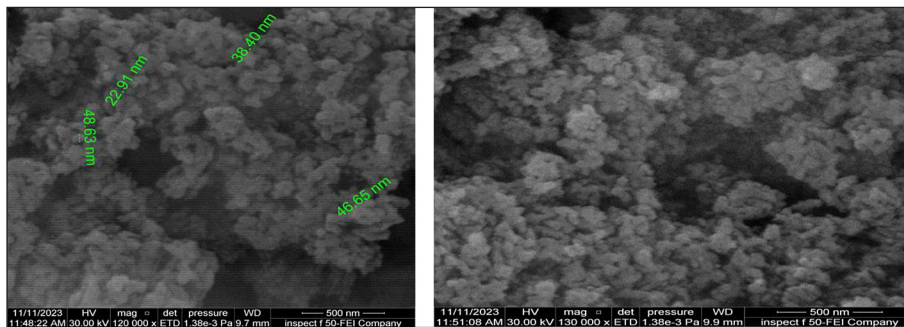**Figure 13.** SEM imaging of surface morphology of HA coating on surface at different coating voltage

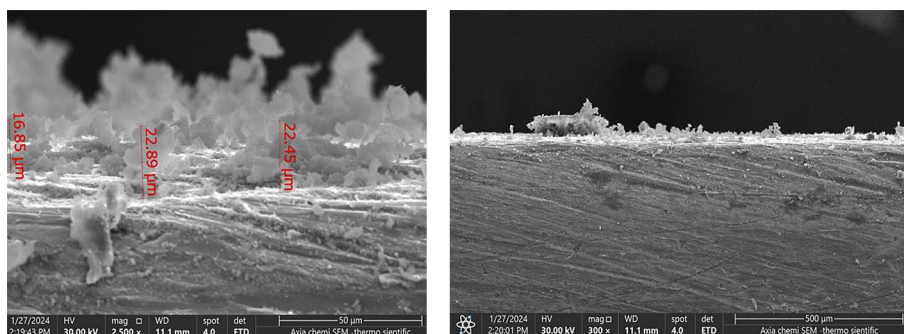**Figure 14.** SEM imaging of HA coating on surface at different particle size

Figure 15. SEM of HA coating thickness

magnification as seen in Figures (12, 13 and 14). Because chitosan is an active binder in the paints, the surface of the paint was smooth and free of holes and fractures. As previously stated by Molaei et al. [21], this aligns with the research. A more uniform coating will result from a more stable suspension. In coated samples, this theory holds true since the suspensions of the coating layer are thought to be the most stable because they have the largest zeta potential values [22, 24] as well as the steadiness of the suspension. The behavior of the coating was impacted by all of the elements described before, but the zeta potential had the most impact [28, 29, 34, 35]. Figure 15 presents SEM of the cross-section of a coated sample to show HA coating thickness.

CONCLUSIONS

Sample mass increase and HA coating thickness are positively correlated with applied voltage and coating time, and better surface coating, when the applied voltage is 40 V and the coating time is five minutes. The thickness of the HA coating obtained in this research, which is the thickness of the coating required for orthopedic implant application was 50–100 μm. Due to the high coating thickness, the surface of the alloy is hydrophilic, which makes the tissue growth on the surface of the alloy more interconnected. This greatly increases biocompatibility, making 316LSS substrates suitable for biomedical applications. Hydroxyapatite coating mixed with chitosan gave new properties, significantly improving osseointegration and reducing the inflammatory effects of implants. The current electrodeposition method has been effectively used to produce HAP/chitosan layer on 316LSS substrates. The highest zeta potential value reached 27.13 mV and a mobility of 2.08 cm^2/Vs for a hydroxyapatite concentration of 7 g/L. The optimal value of the applied voltage is 40 volts, the deposition time is 4 minutes, and the concentration is 7 g/L to obtain good surface coverage.

REFERENCES

1. Ceyhun K. and Kacar R. In vitro bioactivity and corrosion properties of laser beam welded medical grade AISI 316L stainless steel in simulated body fluid, Int. J. Electrochem. Sci., 2016, 11(4), 2762–2777.

2. Neirinck B., Fransaer J., Van der Biest O., and Vleugels J. Aqueous electrophoretic deposition in asymmetric AC electric fields (AC–EPD), Electrochem. commun., 2009, 11(1), 57–60.

3. Goodman S.B., Yao Z., Keeney M., and Yang F. The future of biologic coatings for orthopaedic implants, Biomaterials, 2013, 34(13), 3174–3183.

4. Chew K.-K., Zein S.H.S., Ahmad A. L., McPhail D.S., and Abdullah M.F. The electrochemical studies of the corrosion resistance behaviour of hydroxyapatite coatings on stainless steel fabricated by electrophoretic deposition, J. Ind. Eng. Chem., 2013, 19(4), 1123–1129.

5. Soundrapandian C., Bharati S., Basu D., and Datta S. Studies on novel bioactive glasses and bioactive glass–nano-HAp composites suitable for coating on metallic implants, Ceram. Int., 2011, 37(3), 759–769.

6. Farnoush H., Mohandesi J.A., Fatmehsari D.H., and Moztarzadeh F. A kinetic study on the electrophoretic deposition of hydroxyapatite–titania nanocomposite based on a statistical approach, Ceram. Int., 2012, 38(8), 6753–6767.

7. Xiao Y., Song L., Liu X., Yi J. Nanostructured bioactive glass–ceramic coatings deposited by the liquid precursor plasma spraying process, Appl. Surf. Sci., 2011, 257(6), 1898–1905.

8. Floristán M., Fontarnau R., Killinger A., and Gadow R. Development of electrically conductive plasma sprayed coatings on glass ceramic substrates, Surf. Coatings Technol., 2010, 205(4), 1021–1028.

9. Wei X., Xi T., Zheng Y., Zhang C., and Huang W. In vitro comparative effect of three novel borate bioglasses on the behaviors of osteoblastic MC3T3-E1 cells, J. Mater. Sci. Technol., 2014, 30(10), 979–983.

10. Rahaman M.N., Bal B.S., and Huang W. Emerging developments in the use of bioactive glasses for treating infected prosthetic joints, Mater. Sci. Eng. C, 2014, 41, 224–231,

11. Jia W.-T., Zhang X., Zhang C.-Q., et al. Elution characteristics of teicoplanin-loaded biodegradable borate glass/chitosan composite, Int. J. Pharm., 2010, 387(1–2), 184–186.

12. Stoch A., Brożek A., Kmita G., Stoch J., Jastrzębski W., and Rakowska A. Electrophoretic coating of hydroxyapatite on titanium implants, J. Mol. Struct., 2001, 596(1–3), 191–200.

13. Yoon D. H. and Muksin K. Alternating current electrophoretic deposition (AC-EPD) of SiC nanoparticles in an aqueous suspension for the fabrication of SiCf/SiC composites, Dig. J. Nanomater. Bios., 2015, 10, 1103,

14. Seuss S., Lehmann M., and Boccaccini A. R. Alternating current electrophoretic deposition of antibacterial bioactive glass-chitosan composite coatings, Int. J. Mol. Sci., 2014, 15(7), 12231–12242.

15. Duta L. and Popescu A. C. Current status on pulsed laser deposition of coatings from animal-origin calcium phosphate sources, Coatings, 2019, 9(5), 335.

16. Mahmoodi S., Sorkhi L., Farrokhi-Rad M., and Shahrabi T. Electrophoretic deposition of hydroxyapatite–chitosan nanocomposite coatings in different alcohols, Surf. Coatings Technol., 2013, 216, 106–114.

17. Eliaz N. and Metoki N. Calcium phosphate bioceramics: A review of their history, structure, properties, coating technologies and biomedical applications, Materials. 2017, 10, 334.

18. Abbass M. K., Khadhim M. J., Jasim A. N., and Issa M. J. A Study the Effect of Porosity of Bio-active Ceramic Hydroxyapatite Coated by Electrophoretic Deposition on the Ti6Al4V Alloy Substrate, in Journal of Physics: Conference Series, IOP Publishing, 2021, 12035.

19. Hazim M. Optimizing of Electrophoretic Deposition and Characterization of Nanobiocomposites Functionally Graded Hydroxyapatite-Yttria Partially Stabilized Zirconia. University of Technology 2017 phd, Thesis.

20. Iman Adnan Anoon, Advance Coating on 316L Stainless Steel Substrate Using an Electrophoretic Deposition for Biomedical Application. phd thesis University of Technology.

21. Sorkhi L., Farrokhi M., Shahrabi T. Electrophoretic deposition of hydroxyapatite chitosan–titania on stainless steel 316 L. Surfaces 2019, 2,458–467.

22. Nuswantoro N., Juliadmi D., Fajri H., Budiman A., Manjas M. Hydroxyapatite Coatings on titanium alloy TNTZ using electrophoretic deposition. Materials Science and Engineering, 2019, 602, 1–12.

23. Drevet R., Ben Jaber N., Fauré J., Tara A., Ben Cheikh Larbi A., and Benhayoune H. Electrophoretic deposition (EPD) of nano-hydroxyapatite coatings with improved mechanical properties on prosthetic Ti6Al4V substrates, Surf. Coatings Technol., 2016, 301, 94–99, https://doi.org/10.1016/j.surfcoat.2015.12.058

24. Chen Q., Liu Y., Yao Q.Q., Yu S.S., Zheng K., Pishetesriedr M., Boccacini A.R. Multilayered bioactive coatings with drug delivery capability by electrophoretic deposition combined with layer by layer deposition, Advanced Biomaterials and Devices in Medicine, 2014, 1, 18–27.

25. Frantiska F., Esther M., Begona F. Electrophoretic deposition of gelatin/hydr-oxyapatite composite coatings onto a stainless steel substrate, Engineering Materials, 2015, 654, 195–199.

26. Minhas B., Hanif Z., Nadeem M.H., et al., The electrochemical and in-vitro study on electrophoretic deposition of chitosan/gelatin/hydroxyapatite coating on 316L stainless steel, Carbohydr. Polym. Technol. Appl., 2023, 5, 100322.

27. Nuswantoro N.F., Budiman I., Septiawarman A., Tjong D.H., and Manjas M. Effect of Applied Voltage and Coating Time on Nano Hydroxyapatite Coating on Titanium Alloy Ti6Al4V Using Electrophoretic Deposition for Orthopaedic Implant Application, in IOP Conference Series: Materials Science and Engineering, IOP Publishing, 2019, 12004.

28. Jasim A.N., Khethier Abbass M., Jasim M., and Salah K. Synthesis, Characterization and Optimization of Electrophoretic Deposition (EPD) Parameters of YSZ Layer on Ti-6Al-4V Alloy substrate, in IOP Conference Series: Materials Science and Engineering, IOP Publishing, 2020, 12082.

29. Abbass M.K., Khadhim M.J., Jasim A.N., Issa M.J., and Khashan K.S. Fabrication and optimization of electrophoretic deposition parameters using alternating current by Taguchi design, Al-Nahrain J. Eng. Sci., 2021, 24(1), 8–15.

30. Hussein, Marwan B., Ali M. Mustafa, and Makarim H. Abdulkareem. A Comparative Study on Dip Coating and Corrosion Behavior of Ti-13Zr-13Nb and Commercially Pure Titanium Alloys Coated with YSZ by Taguchi Design." Salud, Ciencia y Tecnología-Serie de Conferencias 2024, 3, 847–847.

31. Hussein, Marwan B., Ali M. Mustafa, Makarim H. Abdulkareem, and Ahmed A. Alamiery. Comparative corrosion performance of YSZ-coated Ti-13Zr-13Nb alloy and commercially pure titanium in orthopedic implants. South African Journal of Chemical Engineering 2024, 48, 40–54.

32. Salman J.M. and Aziz M.L. Some properties of biomedical Ti6al4v alloy in different solutions, Iraqi J. Mech. Mater. Eng., 2019, 19(2), 138–156.

33. Al-Bawee A., Khodair Z.T., Hussein A.K., and Jasim A.N. Enhancing biocompatibility and osseointegration of medical implants using ti based nanocomposite coatings, Multidiscip. Sci. J., 2024, 6(9), 2024183.

34. Wu A., Vilarinho P.M., and Kingon A.I. Electrophoretic deposition of lead zirconate titanate films on metal foils for embedded components, J. Am. Ceram. Soc., 2006, 89(2), 575–581.

35. Hussein, Marwan B., Ali M. Mustafa, and Makarim H. Abdulkareem. A comparative study on dip coating and corrosion behavior of Ti-13Zr-13Nb and commercially pure titanium alloys coated with YSZ by Taguchi design. Salud, Ciencia y Tecnología-Serie de Conferencias 3, 2024, 847–847.